Process outgrowth in oligodendrocytes is mediated by CNP, a novel microtubule assembly myelin protein

John Lee,[1] Michel Gravel,[1] Rulin Zhang,[2] Pierre Thibault,[3] and Peter E. Braun[1]

[1]Department of Biochemistry, McGill University, Montreal, Quebec H3G 1Y6, Canada
[2]WEMB Biochem, Inc., Toronto, Ontario M9W 1E7, Canada
[3]Institut de Recherches en Immunologie et Cancer, Université de Montréal, Montreal, Quebec H3C 3J7, Canada

Oligodendrocytes (OLs) extend arborized processes that are supported by microtubules (MTs) and microfilaments. Little is known about proteins that modulate and interact with the cytoskeleton during myelination. Several lines of evidence suggest a role for 2′,3′-cyclic nucleotide 3′-phosphodiesterase (CNP) in mediating process formation in OLs. In this study, we report that tubulin is a major CNP-interacting protein. In vitro, CNP binds preferentially to tubulin heterodimers compared with MTs and induces MT assembly by copolymerizing with tubulin. CNP overexpression induces dramatic morphology changes in both glial and nonglial cells, resulting in MT and F-actin reorganization and formation of branched processes. These morphological effects are attributed to CNP MT assembly activity; branched process formation is either substantially reduced or abolished with the expression of loss-of-function mutants. Accordingly, cultured OLs from CNP-deficient mice extend smaller outgrowths with less arborized processes. We propose that CNP is an important component of the cytoskeletal machinery that directs process outgrowth in OLs.

Introduction

Oligodendrocytes (OLs) are myelinating cells in the central nervous system. In early myelinogenesis, OLs elaborate highly branched processes that target and wrap axons to form the myelin sheath, which is a specialized membrane that is essential for promoting rapid propagation of action potentials by saltatory conduction. The important role of OLs is critically dependent on the establishment of their arborized morphology, which is supported by the cytoskeleton that consists of microtubules (MTs) and microfilaments but not intermediate filaments (Wilson and Brophy, 1989). Recent studies provided important insights into MT organization (Lunn et al., 1997) and coordinated MT and microfilament reorganization during process outgrowth and branch formation (Song et al., 2001a). However, the molecular mechanisms and identities of cytoskeleton-interacting proteins that mediate process outgrowth in OLs remain poorly defined.

One potential candidate for coordinating cytoskeleton reorganization during process formation is 2′,3′-cyclic nucleotide 3′-phosphodiesterase (CNP), a prenylated myelin protein that is highly expressed in OLs (for review see Braun et al., 2004). CNP binds to MTs and exhibits MT polymerization activity in vitro (Laezza et al., 1997; Bifulco et al., 2002). In addition, CNP may associate directly with F-actin (Dyer and Benjamins, 1989; De Angelis and Braun, 1996). During development, CNP expression is highly up-regulated in premyelinating OLs before the commencement of myelination and is maintained throughout life (Scherer et al., 1994). Although the function of CNP is unknown, this expression pattern suggests an important role for CNP in the myelination process as well as for the lifelong maintenance of the myelin sheath. This is supported by cell biological and genetic studies linking CNP to process extension events. Premyelinating OLs in CNP-overexpressing mice extend redundant and aberrant membranous extensions from their processes, periaxonal membranes, and contact points between processes and myelin internodes (Gravel et al., 1996; Yin et al., 1997). Adult OLs from these transgenic animals regrow dramatically larger and more extensively branched processes in culture. In addition, ectopic CNP expression in fibroblasts induces membrane expansion and formation of filopodia and processes (De Angelis and Braun, 1994). In contrast, CNP-null mice appeared to myelinate normally but suffered severe neurodegeneration from axonal loss with increasing age (Lappe-Siefke et al., 2003). Further analysis revealed that CNP deficiency caused major abnormalities to the structure of the paranodal loops of mice OLs as early as 3 mo of age, which is before any visible onset of axonal degeneration (Rasband et al., 2005). Because paranodal loops contact the axolemma for axon–glial signaling, which is critical for axonal

Correspondence to John Lee: johnlee@gene.com

Abbreviations used in this paper: CF, catalytic fragment; CMV, cytomegalo virus; CNP, 2′,3′-cyclic nucleotide 3′-phosphodiesterase; MAP, MT-associated protein; MT, microtubule; MTOC, MT-organizing center; OL, oligodendrocyte; RSV, rous sarcoma virus.

The online version of the article contains supplemental material.

The Journal of Cell Biology, Vol. 170, No. 4, August 15, 2005 661–673
http://www.jcb.org/cgi/doi/10.1083/jcb.200411047

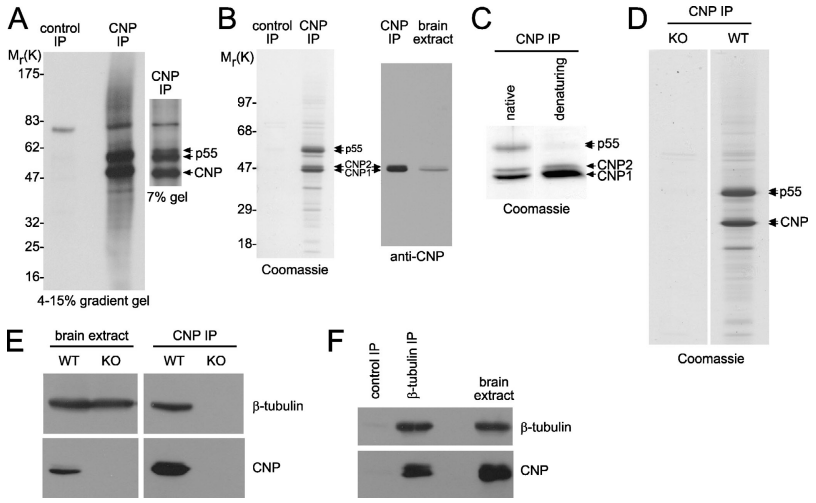

Figure 1. **Identification of tubulin as a major CNP-interacting protein.** (A) Coimmunoprecipitation of p55 from cultured OLs. Autoradiography of metabolic-labeled OL extracts immunoprecipitated (IP) with control or CNP mAbs on 4–15% sucrose gradient (left) and 7% SDS-PAGE gel (right). (B) Copurification of p55 from whole brain extracts. Coomassie staining (left) and CNP immunoblot (right) of rat brain extracts immunoprecipitated with cross-linked control or CNP mAb beads on a 4–15% sucrose gradient gel. M_r(K), mol wt in kD. (C) CNP immunoprecipitation of native and denatured rat brain extracts. (D and E) CNP immunoprecipitation of brain extracts from wild-type (WT) and CNP knockout (KO) mice were analyzed by Coomassie staining (D) and CNP and β-tubulin immunoblots (E). (F) Reverse coimmunoprecipitation of CNP with β-tubulin antibody. Rat brain extracts were immunoprecipitated with cross-linked control or β-tubulin mAb beads and were analyzed by β-tubulin and CNP immunoblots.

integrity and organization (Salzer, 2003), neurodegeneration is a secondary consequence of OL defects and impaired cell–cell communication. To elucidate the function of CNP in OLs, we sought to identify its physiological binding partners. In this study, we demonstrate that CNP interacts with tubulin heterodimers and promotes MT assembly. Furthermore, CNP induces MT and F-actin reorganization, which are necessary for process outgrowth and arborization in OLs.

Results

Identification of tubulin as a major CNP-interacting protein

To identify CNP-interacting proteins, we immunoprecipitated CNP from [^{35}S]methionine-labeled cultured rat OLs and resolved proteins on 4–15% sucrose gradient gels. A predominant 55-kD polypeptide (p55) copurified with CNP, both of which did not precipitate with the control antibody (Fig. 1 A). Optimal resolution on a 7% SDS-PAGE gel revealed p55 as a doublet. Because p55 and CNP migrated closely with IgG heavy chains, we used antibody-coupled beads. p55 coimmunoprecipitated with both CNP isoforms from rat brain homogenate in a 1:1 ratio, as shown by Coomassie staining (Fig. 1 B). A western blot probed with the same CNP immunoprecipitation antibody demonstrated that p55 was not isolated because of antibody cross reactivity. Moreover, p55 failed to purify with CNP from denatured brain extracts (Fig. 1 C), and both proteins, as well as many other protein bands, were absent upon immunoprecipitation of brain homogenate from CNP-null mice (Fig. 1 D), indicating that p55 interacts with CNP. Predominant silver-stained bands were excised and subjected to trypsin proteolysis and mass spectrometry for protein identi-

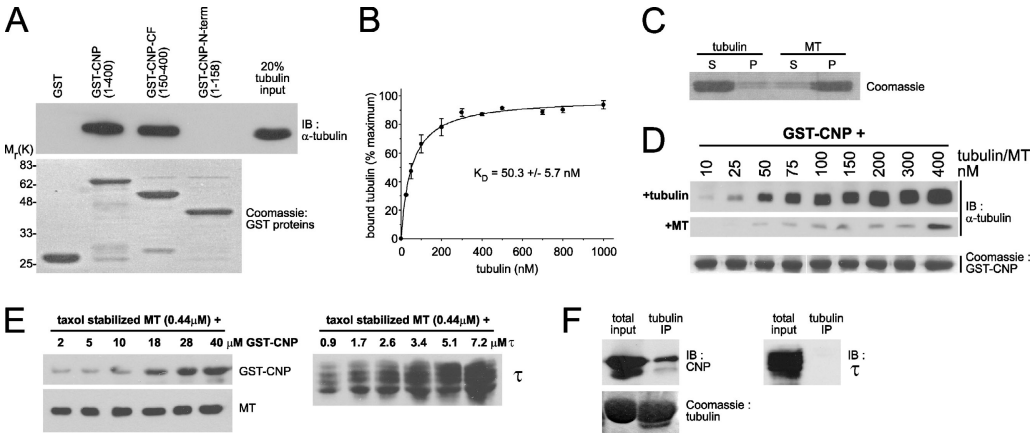

Figure 2. **CNP binds more preferentially to tubulin than preassembled MTs in vitro.** (A) Tubulin binding assay. 1 μM GST-CNP deletion mutants were incubated with 0.1 μM tubulin and 20 μl glutathione–Sepharose beads. Bound tubulin was analyzed by immunoblotting (IB) for α-tubulin (top). Coomassie-stained purified GST-CNP proteins (bottom). M_r(K), mol wt in kD. (B) Quantitative analysis of tubulin binding to GST-CNP. Various concentrations of tubulin (25 nM–1 μM) were added to 13 nM GST-CNP for binding. Bound tubulin (y axis) was quantified by densitometry and plotted as a function of tubulin concentration (x axis). Results from three independent experiments were used to calculate the binding constant by nonlinear regression analysis. Error bars represent SD. (C) The assembly state of soluble tubulin and preformed taxol-stabilized MTs was verified for its enrichment in the supernatant (S) and pellet (P), respectively. (D) Comparative binding of soluble tubulin and preassembled MTs to GST-CNP. Various concentrations of preassembled MTs or soluble tubulin (10–400 nM) were added to 2 μM GST-CNP. Bound proteins were analyzed by Coomassie staining and α-tubulin immunoblots. (E) Comparison of CNP and τ binding to MTs. Different amounts of GST-CNP (left) and τ (right) were cosedimented with preassembled MTs and analyzed by immunoblotting. (F) Comparison of CNP and τ binding to tubulin. 9 μM of preloaded tubulin beads were incubated with 0.9 μM GST-CNP (left) or τ (right) and were washed, and immunoprecipitates were analyzed by Coomassie staining and immunoblotting.

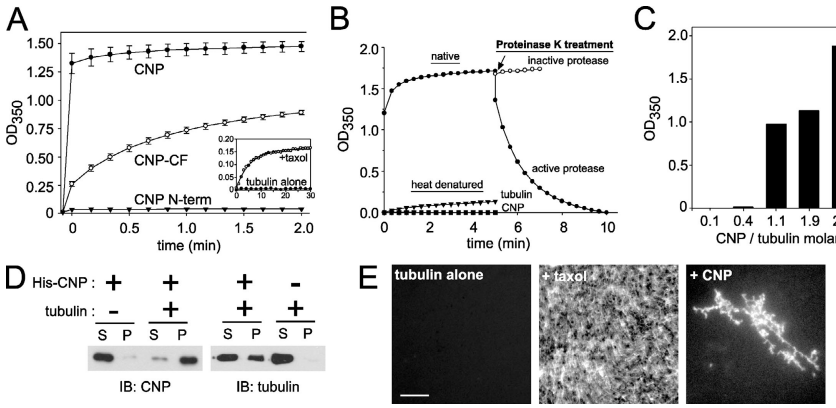

Figure 3. **CNP promotes MT assembly in vitro.** (A) 5 μM His-CNP (closed circles), 5 μM His-CNP–CF (open circles), and 50 μM His-CNP NH_2-terminal region (triangles) were incubated with 5 μM tubulin at 22°C and were OD_{350} monitored. Tubulin alone (closed circles) or in the presence of 50 μM taxol (open circles) is shown in the inset graph. Error bars represent SD. (B) 17 μM His-CNP (closed circles) was incubated with 5 μM tubulin at 22°C and was OD_{350} monitored. After 5 min, 16 μg proteinase K (closed circles) or inactivated proteinase K (open circles) was added to the reaction and was OD_{350} measured for an additional 5 min. No significant polymerization was observed when either component (tubulin, triangles; or His-CNP, squares) was heat denatured. (C) Various amounts of His-CNP were incubated with 5 μM tubulin at 22°C. Differential OD_{350} absorbances for the first 3 min were reported, after which no increases were observed. (D) MT sedimentation assays. 2.2 μM His-CNP was incubated with or without 1.8 μM tubulin at 37°C for 1 h. After sedimentation, supernatants (S) and pellets (P) were analyzed by CNP and tubulin immunoblots (IB). (E) Visualization of polymerized MTs. 9 μM rhodamine-labeled tubulin incubated alone, with 18 μM CNP, or with 50 μm taxol at 37°C for 30 min was analyzed by immunofluorescence. Bar, 10 μm.

fication by searching measured peptide masses against databases. The p55 doublet corresponded to α- and β-tubulin, as shown by tubulin copurification from wild-type, but not CNP-null, mice brain extracts (Fig. 1 E). Moreover, CNP and tubulin interactions were demonstrated by reverse coimmunoprecipitation of CNP with the β-tubulin antibody (Fig. 1 F).

CNP binds preferentially to tubulin heterodimers compared with MTs in vitro

To assess CNP interaction with tubulin heterodimers, GST pull-down assays were performed using recombinant GST-CNP deletion mutants incubated with tubulin under conditions that prevent MT polymerization (very low tubulin concentration, 4°C incubation, and an absence of Mg and GTP). Tubulin bound to CNP and the COOH-terminal fragment (CNP–catalytic fragment [CF]; residues 150–400) but not to the NH_2-terminal region (CNP–NH_2 terminal; residues 1–158; Fig. 2 A). Tubulin remained associated with CNP even after extensive high salt washes (2 M NaCl; unpublished data). The binding affinity of GST-CNP for tubulin was saturable with an apparent K_d of 50.3 ± 5.7 nM (Fig. 2 B).

To assess CNP binding to MTs, we compared relative amounts of taxol-stabilized MTs with tubulin heterodimers that were retained by GST-CNP. The assembly state of tubulin and taxol-polymerized MTs that were used for binding experiments was initially verified by sedimentation analysis (Fig. 2 C). As shown in Fig. 2 D, fewer MTs bound to CNP compared with tubulin; however, the binding affinity for MTs could not be determined at the low concentration range that was examined (10–400 nM). Consistent with this, we also noted that in our procedure to purify tubulin from brain tissue, CNP, unlike other MT-associated proteins (MAPs; MAP2 and τ), failed to copurify with MTs that were isolated by two successive assembly/disassembly cycles (unpublished data). To further substantiate preferential binding of CNP to tubulin heterodimers, we performed MT cosedimentation assays (Fig. 2 E). GST-CNP exhibited weaker affinity for taxol-polymerized MTs with an apparent K_d of 11.0 ± 2.1 μM, which is ~220-fold higher than that for soluble tubulin. In comparison with CNP, τ possessed greater affinity for MTs (K_d of 1.24 ± 0.3 μM), which is similar to previous measurements (~1 μM; Gustke et al., 1994). When we extended our analysis to compare CNP and τ binding with soluble tubulin (Fig. 2 F), GST-CNP, but not τ as expected (Fukata et al., 2002), bound to tubulin-preloaded beads. Our results show that CNP is different from MAPs, binding preferentially to tubulin heterodimers compared with MTs in vitro.

CNP copolymerizes with tubulin and induces MT assembly in vitro

CNP exhibits MT polymerization activity in vitro (Bifulco et al., 2002). To identify the MT assembly domain, we incubated His-CNP deletion mutants with tubulin and assessed polymerization by monitoring increasing solution turbidity over time. Both CNP and CNP-CF induced tubulin polymerization (Fig. 3 A). The larger assembly effect of the full-length protein suggests synergistic contribution of the NH_2-terminal region for polymerization, although the COOH-terminal domain itself sufficiently mediates tubulin binding and MT assembly. On the other hand, no turbidity was observed with tubulin alone (Fig. 3 A, inset), CNP alone (not depicted), or with either heat-denatured components (Fig. 3 B). Moreover, the addition of protease after the assembly reaction eliminated turbidity (Fig. 3 B). These control experiments demonstrate that polymerization is dependent on native CNP and tubulin interactions. To assess the concentration dependency for polymerization, varying amounts of CNP were incubated with tubulin. Equimolar high concentrations of CNP were required to elicit polymerization (Fig. 3 C), suggesting that it initially binds to tubulin dimers to form MTs. Indeed, when CNP was incubated with tubulin and pelleted by centrifugation, CNP was recovered predominantly in the MT pellet, indicating that it copolymerizes with tubulin (Fig. 3 D). To visualize MT formation, we incubated rhodamine-labeled tubulin with CNP and examined the reaction products by fluorescence microscopy. Although taxol stimulated the assembly of small, thin MT strands, CNP formed large tubulin aggregates and dramatically longer and thicker bundled MT strands (Fig. 3 E) even after brief incubation (37°C for 1 min) or at low temperatures (22°C for 30 min). In addition, based on the bio-

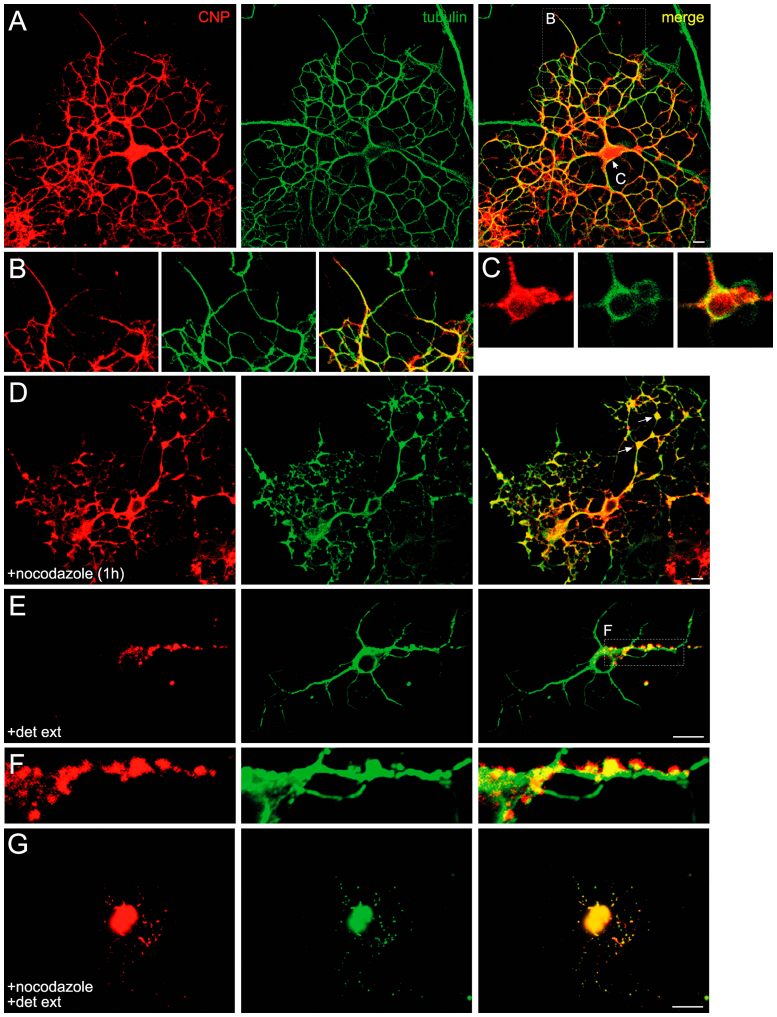

Figure 4. **CNP colocalizes with tubulin/dynamic MTs in cultured OLs.** Cells were double stained for CNP (red) and tubulin (green). (A) Mature OL. Magnified regions of the processes and cell body are shown as insets B and C, respectively. (B) CNP colocalizes extensively with tubulin/MTs in a subset of processes. (C) The image of the cell body was obtained at a lower intensity and at a higher focal plane. CNP colocalizes with cortical MTs in the cell body. (D) Cells treated with 10 μg/ml nocodazole for 1 h. Even with complete MT depolymerization, as assessed by detergent extraction before fixation (G), CNP colocalizes extensively with tubulin. Cytoplasmic extrusions along the processes, where branching occurs, are swollen (arrows). (E) Cells preextracted with detergent in MT-preserving buffer before fixing. A magnified view of the main process is shown as inset F, where CNP/tubulin-enriched varicosities colocalize with stable MTs. (G) Cells were treated with 10 μg/ml nocodazole for 1 h, and then were detergent extracted before fixing. Only detergent-insoluble varicosities remain. Bars, 10 μm.

chemical property that tubulin dimers hydrolyze GTP efficiently in its assembled state within the MT lattice, a significant high rate of GTP hydrolysis was measured during CNP-mediated assembly, further supporting veritable formation of MTs (Fig. S1, available at http://www.jcb.org/cgi/content/full/jcb.200411047/DC1). Our results collectively demonstrate that CNP mediates strong tubulin polymerization in vitro by binding to tubulin dimers to form MTs and polymeric tubulin structures.

CNP colocalizes predominantly with tubulin/dynamic MTs in cultured OLs

To support our biochemical data, we determined whether endogenous CNP colocalized with tubulin/MTs in cultured OLs that were isolated from neonatal rat brains. OL progenitors were plated and cultured under conditions that enriched for a synchronized population of differentiating cells. During the first 2 d of differentiation, bipolar progenitor cells began to express high levels of CNP and to extend multiple processes to become immature OLs. After further differentiation, mature cells developed large arborized processes (Fig. 4 A). CNP was widely distributed, colocalizing with tubulin/MTs in numerous subsets of branches (Fig. 4 B) and at the cortical edge of the cell body (Fig. 4 C). Significant colocalization was also observed in the cell body and in processes of immature OLs (Fig. S2, available at http://www.jcb.org/cgi/content/full/jcb.200411047/DC1).

Because cells were initially fixed before permeabilization, both MTs and soluble tubulin were effectively labeled by immunostaining with the antitubulin antibody. To ascertain whether CNP colocalized preferentially with MT polymers or tubulin monomers, cells were treated with sufficient nocodazole to depolymerize MTs without causing major process retraction and gross morphological changes. Even with MT depolymerization, CNP colocalized extensively with soluble tubulin, particularly in swollen cytoplasmic extrusions where processes branched (Fig. 4 D, arrows). Depolymerization induced minor process retraction, resulting in a smaller arborized network with jagged branches (Fig. 4, compare A with D). The structural integrity of OL processes remained supported by the unperturbed F-actin cytoskeleton; concomitant cytochalasin treatment severely disrupted most branching (unpublished data).

Conversely, we also asked whether CNP colocalized with stable MTs in cells that were preextracted with MT-stabilizing buffer containing 1% Triton X-100 to remove soluble tubulin and dynamic unstable MTs before fixing (Song et al., 2001a). As expected, stable MTs in the cell body and main processes, but not in smaller branches, were preserved (Fig. 4 E). This is in contrast with cells that were pretreated with nocodazole to

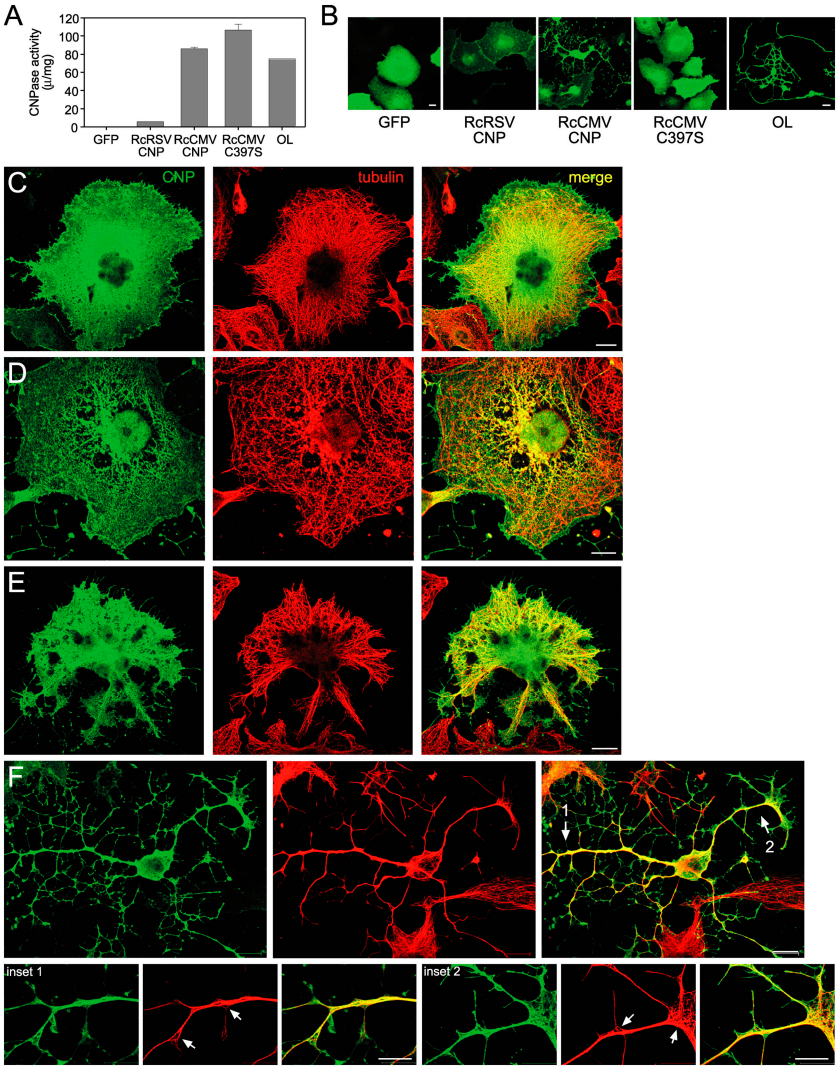

Figure 5. **CNP overexpression in COS-7 cells induces OL-like process outgrowth.** (A) Comparison of CNP expression levels. Similar transfection efficiencies were achieved for each construct by immunofluorescence assessments. CNP expression in RcCMV-CNP–transfected cells is comparable with endogenous levels in cultured OLs. Error bars represent SD. (B) Transfected cells in A are depicted using the same image settings. (C–F) RcCMV-CNP–transfected cells exhibiting various morphology changes are shown double stained for CNP (green) and tubulin (red). Magnified regions in F are shown as insets, where MTs are splayed in cytoplasmic extrusions along the processes (insets 1 and 2, arrows). Bars, 10 μm.

depolymerize all MTs before detergent extraction (Fig. 4 G). In both cases, CNP was almost completely extracted except for detergent-insoluble varicosities, which were enriched for CNP and tubulin and appeared to be associated with stable MTs (Fig. 4 F). The existence of insoluble structures correlate with earlier observations reporting a subpopulation of CNP in the detergent-insoluble cytoskeleton that is enriched for tubulin from cultured OLs and brain tissue (Pereyra et al., 1988; Gillespie et al., 1989; Wilson and Brophy, 1989). These structures could, in fact, be large vesicular complexes that are transported along MTs for process outgrowth. Our overall results suggest that CNP associates preferentially with soluble tubulin and dynamic MTs as opposed to stable MTs in vivo.

CNP overexpression promotes OL-like arborized process formation in COS-7 cells

CNP overexpression in fibroblasts induces filopodia and process formation (De Angelis and Braun, 1994), presumably by modulating the F-actin cytoskeleton (De Angelis and Braun, 1996). We sought to determine whether these effects are also attributable to CNP interactions with tubulin/MTs. COS-7 cells were transfected with either Rc rous sarcoma virus (RSV)–CNP or Rc cytomegalo virus (CMV)–CNP constructs for low and high CNP expression, respectively, yielding a 17-fold difference in CNP levels with similar transfection efficiencies (Fig. 5 A). In comparison with cells expressing GFP, RcRSV-CNP–transfected cells exhibited minor morphology changes and produced some filopodia (Fig. 5 B). In contrast, cells transfected with the high expression construct displayed dramatic morphology changes. Similarly high expression levels were measured for endogenous CNP in cultured OLs, as assessed by enzymatic activity (Fig. 5 A) and immunofluorescence intensity measurements (Fig. 5 B). Also noteworthy is the fact that morphology effects are dependent on CNP prenylation, as expected from earlier observations (De Angelis and Braun, 1994); expression of the C397S mutant (lacking a functional CAAX motif) failed to elicit any morphology changes (Fig. 5 B) even at the highest expression levels (Fig. 5 A). Thus, CNP-induced morphology changes are dependent on sufficiently high expression and prenyl-dependent membrane localization.

COS-7 cells that were transfected with the high expression RcCMV-CNP construct exhibited heterogeneous morphologies, collectively representing the transformation process

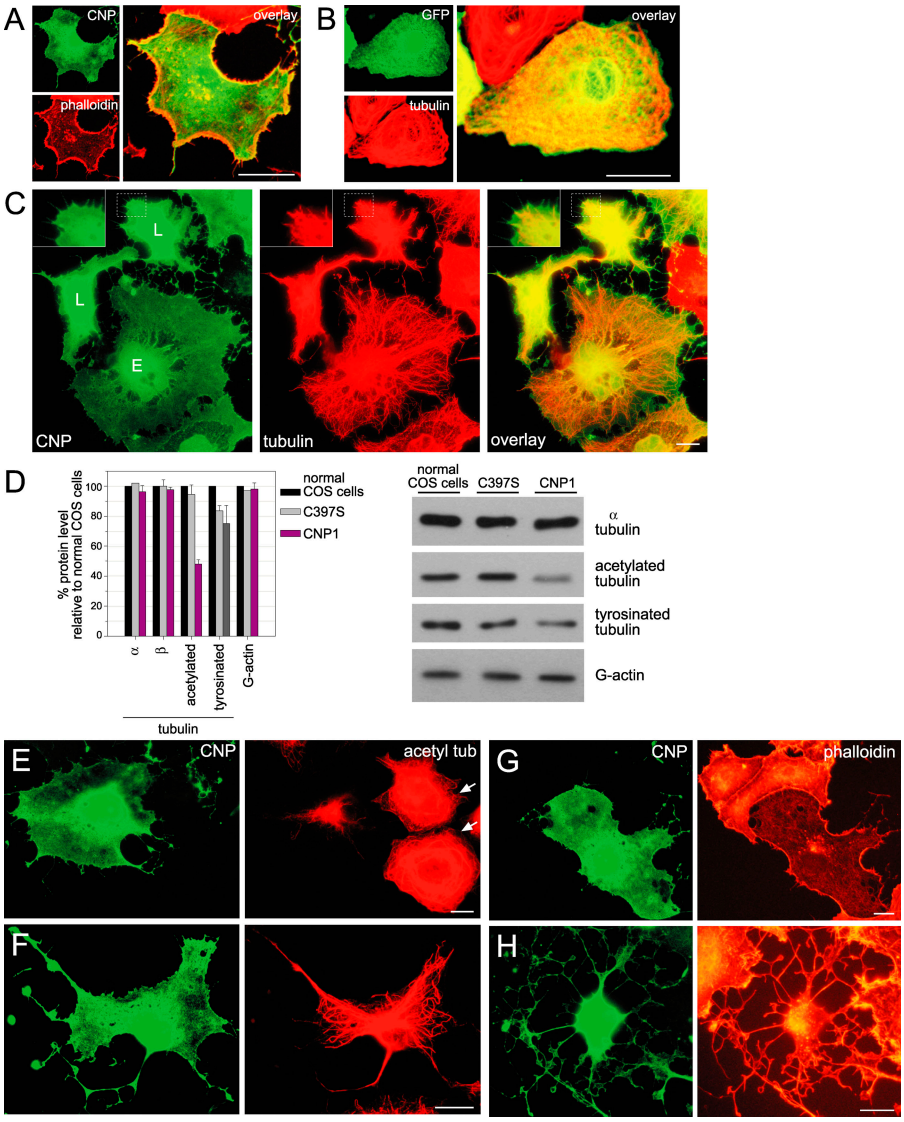

Figure 6. **CNP induces MT and F-actin reorganization in COS-7 cells.** (A–C) Transfected COS-7 cells analyzed by epi-immunofluorescence. Image overlays of CNP and F-actin (A), GFP and tubulin (B), and CNP and tubulin (C). (C) Early stage (E) and late-stage (L) transformed cells. Insets show magnified regions of the cell periphery. (D) Immunoblot analysis of tubulin and G-actin levels in cell extracts. Protein levels, relative to nontransfected cells, were measured by densitometry and were averaged from five independent experiments. Representative blots are shown on the right. (E and F) Cells double stained for CNP and acetylated tubulin. (E) Loss of acetylated MTs in the early stage of transformation. Arrows indicate nontransfected cells. (F) In late-stage transformation, reorganized MTs become stabilized. (G and H) Cells double stained for CNP and F-actin. Loss of cortical actin and stress fibers in CNP-expressing cells at early stage (G) and late-stage (H) transformation. Bars, 20 μm.

leading to the OL-like arborized morphology (Fig. 5 F). Increased cell spreading and filopodial protusions were apparent in less transformed "early stage" cells (Fig. 5 C). Interestingly, some of these cells showed predominant perinuclear CNP localization in the vicinity of the MT-organizing center (MTOC), where many CNP/tubulin-enriched varicosities were distributed along filamentous CNP/MT-colocalized strands that extended radially to the outer periphery (Fig. 5 D). Given that MT growth and transport from the MTOC occurs in neurons during neurite extension (Yu et al., 1993), it is tempting to speculate that these structural features may reflect CNP-mediated tubulin transport to the cell edges, which is necessary for process extension. Further live cell imaging experiments will be required to test our conjecture.

More transformed "late-stage" cells showed major cell shape distortion, MT bundling, and elongation of MT-filled processes (Fig. 5 E). These changes appeared to lead to the OL-like branched morphology (Fig. 5 F). The much smaller cell body extended numerous major processes containing secondary and tertiary branches. CNP colocalized with tubulin/MTs in the larger processes, which were diametrically nonuniform throughout the entire lengths and contained many cytoplasmic extrusions that were sites for additional branching and redirection of splayed MTs (Fig. 5 F, insets 1 and 2, arrows).

CNP induces coordinated reorganization of the MT and F-actin cytoskeleton

We examined changes to the MT network in COS-7 cells in greater detail during CNP-induced transformation by normal epi-immunofluorescence to view the entire cytoskeleton at all focal planes. First, we compared CNP staining relative to that of F-actin to demonstrate that CNP extended to the cell edges and coaligned with cortical actin and filopodia (Fig. 6 A). Image overlays of GFP and tubulin reveal that the MT network in normal COS-7 cells is highly dense with curly MT strands that are in close apposition with the cell margins (Fig. 6 B). In contrast, the area of MT networks in CNP-transformed early stage cells were significantly larger and less dense, with radial reorganization of thicker, bundled MTs and numerous frayed ends pointed toward the cell edge (Fig. 6 C, cell labeled "E"). This

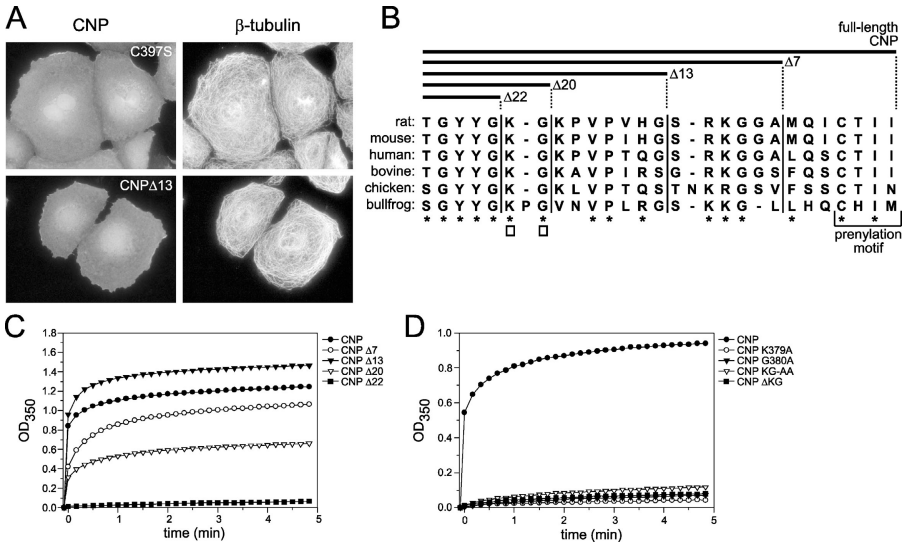

Figure 7. **Tubulin polymerization mutants.** (A) Transfected COS-7 cells expressing C397S (top) and CNPΔ13 (bottom) that are double stained for CNP (left) and tubulin (right). Deletion of the last 13 residues does not affect MT organization. (B) Sequence alignment of the CNP COOH terminus. COOH-terminal deletion mutants are shown above the sequences. Conserved residues are marked as stars. K379 and G380 are indicated by boxes. (C and D) MT polymerization assays. 10 μM CNP deletion mutants (C) and K379 and G380 mutants (D) were incubated with 5 μM tubulin at 22°C and were OD_{350} monitored.

indicated MT reorganization and spreading during the initial stage of morphogenesis. Concordantly, late-stage cells became much smaller, with highly dense MT cytoskeletons (Fig. 6 C, cells labeled "L"). As an initial step in process extension, frayed MT ends appear to invade extended filopodia (Fig. 6 C, insets).

Given the extensive reorganization of MTs, we examined changes to tubulin levels by immunoblot analysis of CNP-transformed cells compared with normal COS-7 cells and non-transformed cells expressing C397S (Fig. 6 D). Although there were no differences in α- and β-tubulin levels, tyrosinated tubulin decreased slightly but to the same extent in both CNP- and C397S-expressing cells. On the other hand, acetylated tubulin levels in CNP-transformed cells decreased by 50% exclusively. Because stable MTs are highly enriched for acetylated tubulin, we wondered if this decrease signified loss of stable MTs during CNP-induced morphogenesis. Indeed, stable MTs were drastically diminished and radially organized in most early stage cells (Fig. 6 E). In more transformed late-stage cells, stable MTs became reestablished with bundled MTs in growing processes (Fig. 6 F). Thus, CNP initially induces MT destabilization, which is necessary for affecting cytoskeletal reorganization for process extension.

Cortical actin and stress fibers structurally reinforce and maintain cell shape, thereby preventing MT protrusion from the cell surface. Along with reorganization of the F-actin cytoskeleton (filopodia and lamellipodia formation), these F-actin barriers must be disrupted to permit process extension, as shown for MAP2-induced process formation in certain nonneuronal cell types (Edson et al., 1993). Not surprisingly, CNP induces F-actin reorganization during morphogenesis. Although total monomeric actin levels were unaltered (Fig. 6 D), phalloidin staining intensities were dramatically reduced in CNP-expressing cells compared with nontransfected cells (Fig. 6, G and H). Stress fibers were absent, and cortical actin was noticeably thinner in localized areas of extruding filopodia and processes. The involvement of F-actin in CNP-induced morphology changes was tested in morphologically less plastic cell types such as HeLa S3 cells, which contain thicker cortical actin and more abundant stress fibers (supplemental material and Figs. S3 and S4, available at http://www.jcb.org/cgi/content/full/jcb.200401147/DC1). Although CNP induced some loss of cortical actin and stress fibers, it failed to promote MT extension and process outgrowth in HeLa S3 cells. However, F-actin disruption using cytochalasin permitted the formation of long, arborized processes in the absence of de novo F-actin assembly. Thus, CNP-mediated process extension is attenuated by F-actin barriers in morphologically less plastic HeLa S3 cells.

Specific COOH-terminal residues are essential for MT polymerization

We wanted to ascertain if CNP-induced morphology changes in COS-7 cells are attributed to its tubulin polymerization activity. It was shown that the 13-residue COOH terminus is essential for MT polymerization in vitro (Bifulco et al., 2002). Moreover, ectopic expression of the COOH-terminal deleted mutant (also lacking the CAAX motif) in COS cells caused severe MT cytoskeleton retraction. It was suggested that CNP is a membrane-bound MAP that anchors MTs to the plasma membrane and may be required for normal MT organization. It is worth noting that there was no description in that study of morphology changes or process formation upon ectopic wild-type CNP expression in COS cells; we presume that this is because of insufficient CNP expression. Therefore, we transfected COS-7 cells with the same CNP deletion mutant construct (CNPΔ13). Although CNPΔ13 failed to elicit any morphology changes, the diffuse cytoplasmic CNP staining pattern looked identical to that of the nonprenylated C397S mutant (Fig. 7 A). Because prenylation is critical for CNP-induced process outgrowth (Fig. 5 B), this suggested to us that the failure of CNPΔ13 to induce morphology changes is attributed instead to its mislocalization with the deletion of the CAAX motif at the COOH-terminal end. Moreover, no retraction of the MT cytoskeleton was observed (Fig. 7 A). It remained unaffected, as it did in cells expressing C397S or GFP (Fig. 6 B), suggesting that CNP is not important for maintaining normal MT distribution in COS cells. This is in alignment with the fact that these cells do not express any detectable endogenous CNP

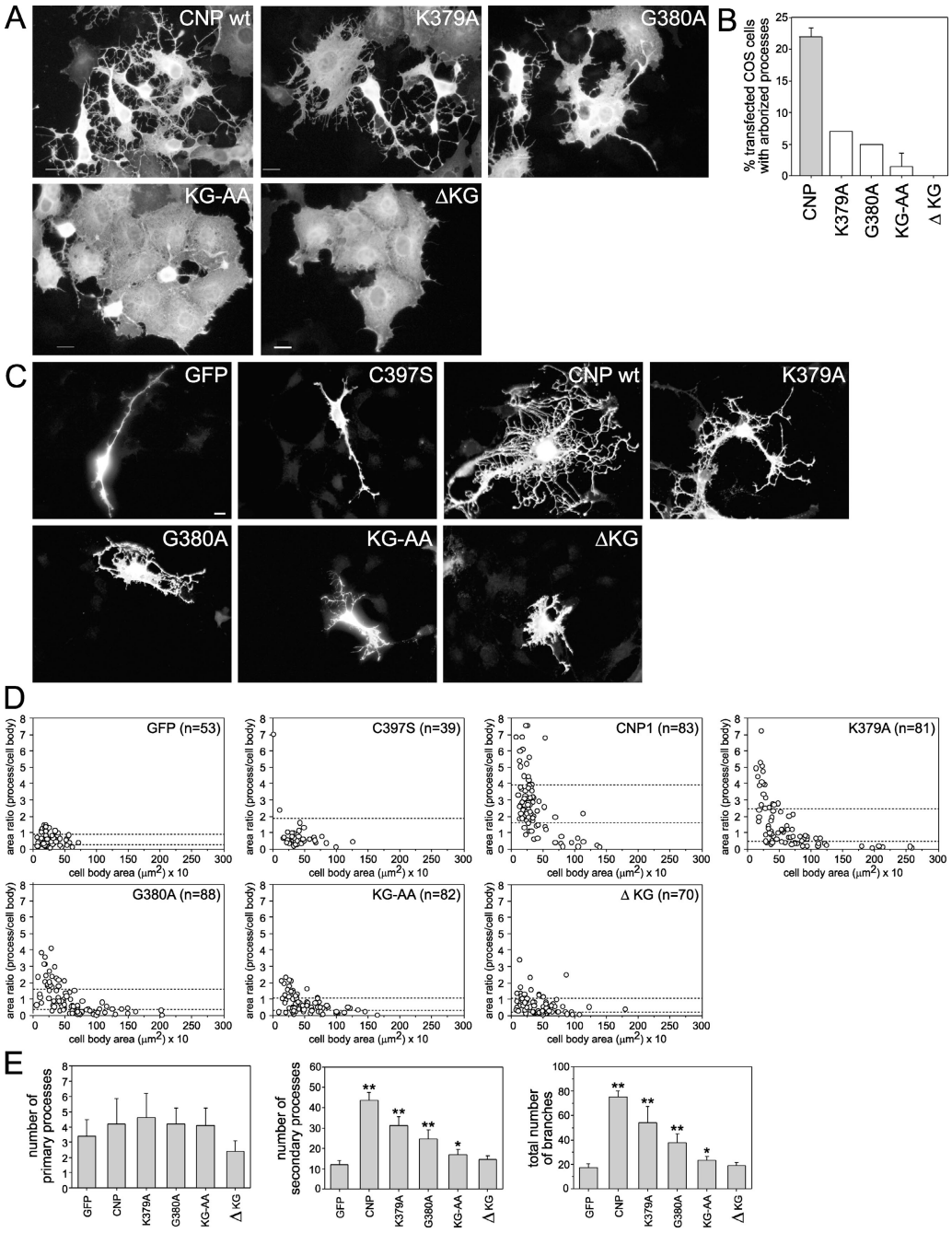

Figure 8. **K379 and G380 mutations inhibit or abolish CNP-mediated outgrowth in both COS-7 and OLN-93 cells.** (A) Representative COS-7 cells expressing CNP mutants were stained for CNP. (B) Transfected COS-7 cells were counted and scored for the presence or absence of MT-filled processes that were longer than the widest cell body diameter ($n > 500$). (C) Transfected OLN-93 cells expressing CNP mutants were stained for CNP. Representative cells with the highest degree of morphological complexity are shown. (D) Process outgrowth area analysis. For each construct, transfected OLN-93 cells with high CNP expression were randomly chosen. For each cell image, the surface area of the cell body (y axis) and the entire cell was measured. Process outgrowth area was calculated from the difference of both values. The extent of arborization was expressed as a ratio of process to cell body surface area (y axis). Dotted lines represent the 95% confidence interval. (E) Morphometric analysis. For each construct, 10–15 transfected OLN-93 cells with high CNP expression were selectively chosen for the highest degree of outgrowth complexity from a total of 100 cells. Each cell image was analyzed for the number of primary (>16 μm), secondary, and tertiary branches (>5 μm). Total branch number is the sum of all primary, secondary, and tertiary branches. *t* test: **, $P < 0.001$; *, $P < 0.05$ (compared with GFP). Error bars represent SD. Bars, 10 μm.

(unpublished data). Finally, no cytoskeletal differences were observed between CNPΔ13 and C397S-transfected cells that were stained for F-actin or acetylated and tyrosinated tubulin (unpublished data).

We screened COOH-terminal deletion mutants for MT polymerization activity in vitro with the aim of identifying and targeting specific residues that are essential for MT assembly while preserving the prenylation motif (Fig. 7 B). Turbidity assays revealed that progressive deletions up to the last 20 residues did not substantially impair tubulin polymerization. However, additional removal of K379 and G380 in CNPΔ22 abolished activity (Fig. 7 C). None of the deletions affected tubulin het-

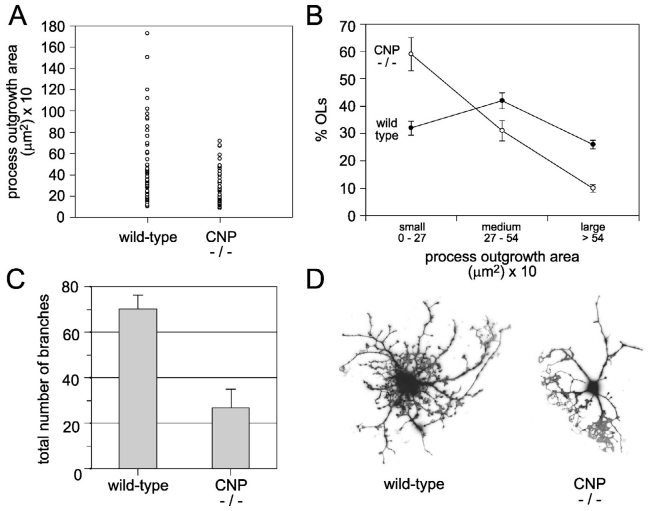

Figure 9. **Decreased process outgrowth and arborization in cultured OLs from CNP-null mice.** Purified OLs from 3-mo-old wild-type and CNP-null mice were plated, treated with 50 ng/ml PMA for 48 h to stimulate process extension, and processed for analysis 5 d afterwards. Cells were double stained for CNP and myelin basic protein. (A) Process outgrowth area analysis. Wild-type (n = 66) and CNP-null OLs (n = 58) were randomly chosen. For each cell image, the process outgrowth area was calculated from the measured values of the total cell and cell body areas. All data were plotted, and the process outgrowth area (y axis) is reflective of the formation of processes and membrane sheets by adult OLs in culture. (B) Data from A are presented to show the relative number of cells with small, medium, or high process outgrowth areas. (C) Morphometric analysis. 10 cells with the largest process outgrowth areas in A were selectively chosen and counted for total number of branches. Error bars represent SD. (D) Representative cells selected for morphometric analysis in C. Myelin basic protein–stained cells are shown as grayscale negatives.

erodimer binding (unpublished data), indicating that only the MT polymerization activity was targeted. Both K379 and G380 are conserved (Fig. 7 B). To assess their importance, we generated recombinant CNP proteins harboring a single mutation (K379A and G380A), double mutation (KG-AA), or an internal K379 and G380 deletion (ΔKG). MT turbidity assays showed significant impairment for all mutants (Fig. 7 D), indicating that K379 and G380 are important for tubulin polymerization in vitro.

K379 and G380 residues are important for process outgrowth and branching

To determine whether the MT polymerization activity of CNP is responsible for the formation of arborized processes, COS-7 cells were transfected with full-length CNP constructs harboring K379 and G380 mutations, and their morphology was analyzed by immunofluorescence. Similar expression levels were detected for wild-type and mutant CNP by immunoblot analysis (unpublished data). As shown in Fig. 8 B, the mutation of either K379 or G380 resulted in 5–7% of cells with arborized morphologies (compared with 22% for wild-type CNP). Additionally, these cells developed fewer processes and branches (Fig. 8 A). These differences were even more pronounced when both residues were mutated or deleted; only 1.5% of KG-AA cells elaborated some form of processes with little or no branching, and none of the ΔKG cells extended any processes.

Because cultured OLs are difficult to transfect and yielded insufficient cell numbers for statistical analysis, we studied the effect of wild-type and mutant CNP expression in the OL cell line, OLN-93, whose bipolar morphology closely resembles O-2A progenitor cells. Given the heterogeneity in cell size and shape within the population, we performed statistical analyses to quantify morphology changes. First, transfected cells for each construct were randomly chosen (identified by GFP or CNP staining), and the surface areas of the entire cell and cell body were measured. The surface area of the processes was calculated by subtracting the two values and was expressed as a ratio of the cell body area (Fig. 8 D, y axis). The average CNP-expressing cell formed processes that were more expansive than the cell body, which is in contrast with GFP- and C397S-expressing cells. Single mutations to K379, and to a greater extent G380, impaired process formation; double mutation and deletion of both residues prevented CNP-induced morphology changes. To quantify the morphological complexity of the process, we selected 10–15 cells with the largest outgrowths for each construct and measured the number of branch types. Representative cells are depicted for each construct in Fig. 8 C. Although wild-type CNP did not affect the number of primary processes in OLN-93 cells, there were many more secondary processes and branching (Fig. 8 E). Similar to our area analysis, single mutations resulted in decreased arborization, whereas double mutation and deletion of both residues negated the complex branching effect. These results demonstrate that K379 and G380 are important for CNP-mediated MT assembly, which is necessary for process branching in OLs.

CNP is essential for process outgrowth in OLs

Neurodegeneration and axonal loss in CNP-deficient mice is caused by paranodal loop defects that impair axon–glial signaling, which is critical for proper axon development and homeostasis (Rasband et al., 2005). Malformation of the paranodal loops may be ascribed to defects in the outgrowth of processes in the absence of CNP. To test this idea, we assessed the ability of OLs that were isolated from 3-mo-old CNP-null mice to regrow processes in culture. Morphological defects of the paranodal loops were initially observed in these mice before the onset of axonal degeneration (Rasband et al., 2005). Purified OLs from wild-type and CNP-null mice were initially stimulated with phorbol ester for 48 h after plating, because adult cells readily regrow processes and membrane sheets in culture only after PKC stimulation or on top of an astrocyte bed layer (Yong et al., 1991; Oh and Yong, 1996). 5 d after phorbol ester treatment, process outgrowth areas of randomly chosen cells were measured, revealing a general deficiency of OLs from CNP-null mice to form processes compared with wild-type cells (Fig. 9 A). Classification of OLs based on their process areas showed that fewer cells from CNP-null mice elaborated large outgrowth areas (26% of wild-type vs. 10% of CNP-null OLs; Fig. 9 B). To quantify the morphological complexity of the processes, we analyzed 10 cells with the largest outgrowth areas and measured the length and number of branches. As depicted by representative cells in Fig. 9 D, the total number of branches

was significantly reduced in CNP-null OLs (70.3 branches in wild-type vs. 26.8 in CNP-null OLs; Fig. 9 C). In contrast, the mean number and length of primary processes were similar (unpublished data). Overall, our results suggest that CNP mediates tubulin polymerization that is necessary for process outgrowth and branching in myelinating OLs.

Discussion

Our data ascribe a biological function for CNP in mediating MT and F-actin reorganization and promoting MT assembly for process outgrowth in OLs. Numerous cytoskeleton-interacting proteins are likely involved in modulating MTs and F-actin along with membrane expansion during myelination. To our knowledge, CNP is the first cytoskeleton effector protein to be described, aside from MAPs, that mediates process outgrowth in OLs.

MAPs bind to MTs to stabilize them against depolymerization (Maccioni and Cambiazo, 1995). Although OLs express MAP2c and τ abundantly, their functional roles remain unclear (Richter-Landsberg, 2001). It was recently shown that Fyn kinase and τ interactions promote process outgrowth in OLs (Klein et al., 2002), and MAP2c is essential for dendritic outgrowth in neurons (Teng et al., 2001; Harada et al., 2002). These findings indicate a general role for both MAPs in branch formation by stabilizing assembling MTs. In contrast, CNP binds preferentially to tubulin heterodimers and copolymerizes with tubulin. Thus, a primary function of CNP is in MT assembly rather than in stabilization, which is in contrast to conventional glial MAPs. Interestingly, CNP is functionally related to two neuronal proteins, CRMP2 (Fukata et al., 2002) and cypin (Akum et al., 2004), both of which bind tubulin dimers and promote assembly in vitro. In vivo, CRMP2 promotes axonal growth and branching, whereas cypin regulates dendrite branching, suggesting that process extension and arborization can be promoted alternatively by tubulin-copolymerizing proteins.

Using COS-7 cells as a model to study cytoskeletal effects (as a result of their large, flat morphology), we examined how CNP transduces changes to the cytoskeleton to promote process outgrowth that is very much similar to OLs. At early stages of morphogenesis, CNP induces MT destabilization, which is necessary for MT reorganization. This is marked by the visible loss of acetylated MTs, which signals increased MT dynamics in the cell. CNP is enriched in the perinuclear region, which comprises the MTOC and is where frequent MT loss is observed. We propose that CNP indirectly disrupts the preexisting MT array by depleting tubulin subunit pools through its interactions with tubulin. In addition, CNP/tubulin varicosities are present and are aligned along radially extended MTs. These varicosities might be CNP/tubulin oligomers that are peripherally transported to cell edges, where MT assembly occurs. Consistent with previous studies, we also observed detergent-insoluble CNP/tubulin varicosities in association with stable MTs in OL processes (Pereyra et al., 1988; Gillespie et al., 1989; Wilson and Brophy, 1989). Whether tubulin is transported exclusively in subunit form or as a stable polymer remains controversial (Baas, 2002; Shah and Cleveland, 2002; Terada, 2003). Interestingly, oligomeric tubulin complexes are transported by kinesin in giant squid axons (Terada et al., 2000). In the absence of pharmacological and live cell imaging studies, we can only speculate that these might be transport elements required for MT assembly. Alternatively, these oligomers may serve as nucleation sites for MT assembly (Caudron et al., 2002). At later stages of morphogenesis, reorganized MTs are stabilized and are marked by the abundant presence of acetylated MTs. Thick, bundled strands are radially projected into the cell periphery, where frayed MT ends extend into filopodia and lamellipodia. As main processes become established, continued MT growth in the processes drives branching. Cytoplasmic extrusions along the processes contain dynamic MTs and are sites for branching, where splayed MTs advance into newly projected F-actin branches. We show that CNP likely promotes MT growth and process arborization by polymerizing MTs at their plus ends. In support of this, process outgrowth is either reduced or abolished in OLs from CNP-null mice as well as in COS-7 and OLN-93 cells overexpressing CNP mutants that are inactive for tubulin polymerization.

CNP also induces F-actin reorganization that is essential for establishing arborized processes by promoting filopodia and lamellipodia formation (De Angelis and Braun, 1994) and causing cortical actin and stress fiber disassembly. F-actin–driven protrusions, in the form of filopodia and lamellipodia, are indispensable for MT growth in neurites and growth cones (Luo, 2002) as well as in developing OL processes (Song et al., 2001a). In contrast, cortical actin can impede MT-driven membrane protusion because it imparts tensile strength to the plasma membrane (Baorto et al., 1992; Edson et al., 1993; Lafont et al., 1993). Stress fibers can also oppose lamellipodia and filopodia formation because cell contractility generally inhibits membrane protrusive activity. Unlike COS-7 cells, both of these F-actin arrays are sufficiently present in HeLa S3 cells to prevent CNP-induced process formation; process extension becomes permissible only upon F-actin disruption using cytochalasin.

CNP's role in process outgrowth appears to be for exclusively myelinating cells, as it is highly expressed only in OLs and Schwann cells. Premyelinating OLs in CNP-overexpressing mice differentiate earlier and produce extraneous membranous extensions at myelin internodes (Gravel et al., 1996; Yin et al., 1997). This gain-of-function phenotype is clearly recapitulated by cultured OLs from adult animals exhibiting faster regrowth of dramatically larger and more complex processes (Gravel et al., 1996). In contrast, CNP-null mice appear to develop normally, showing no apparent myelin abnormalities until 3 mo of age, when paranodal and nodal regions become progressively disorganized (Rasband et al., 2005). With time, these aberrations lead to axonal degeneration (as early as 5 mo) before outward neurodegenerative symptoms develop, eventually leading to premature death (Lappe-Siefke et al., 2003). It is believed that axonal death is directly attributed to improper axon–glial cell signaling and organization that is brought on by the failure to form proper axon–glial contacts at the paranodes. This is highly conceivable in the face of numerous data showing axonal loss as a direct consequence of paranode disorganization (Salzer, 2003).

How does CNP deficiency result in structural defects to the paranodal loops? CNP is an abundant myelin protein, comprising 4% of total CNS myelin proteins by weight. It is widely distributed throughout the OL cell body, processes, and particularly noncompact myelin compartments such as paranodal loops. In ascertaining whether CNP is required for process outgrowth in OLs, we directly assessed the ability of cultured OLs from 3-mo-old CNP-null mice to regrow their processes at an age when paranodal defects first appear. Morphometric and surface area analysis of the processes revealed a significant reduction in process outgrowth and branching, suggesting that loss of CNP affects the MT cytoskeleton, thus causing structural defects to the processes and paranodal loops. The underlying cytoskeleton forms the structural scaffold to support the architecture of the processes and myelin sheath. Like the myelin sheath, the cytoskeleton is continually maintained by protein turnover and synthesis. CNP is likely to be essential for maintaining proper MT organization in the processes and noncompact myelin compartments, possibly by regulating MT assembly and dynamics, transporting tubulin subunits to these sites, and/or stabilizing MTs directly. On the other hand, an aberrant MT cytoskeleton in CNP-null OLs could effectively impede protein transport, affect the assembly of signaling complexes, and/or alter the structure of paranodal loops and other noncompact myelin compartments; all of this could impair axon–glial signaling. For example, the accumulation of dysfunctional MTs in the taiep myelin mutant rat impedes transport of myelin components, leading to the inadequate maintenance of the myelin sheath (Song et al., 2001b).

Similar to the outgrowth of axons and dendrites in neurons, many proteins are likely to contribute to the overall mechanism of process outgrowth in OLs. Although it is clear that CNP is critical for the long-term maintenance of paranodes, additional experiments are planned to address its role in early development during myelination. We reported previously that cultured OL precursors from mutant mice did not exhibit any apparent morphological abnormalities (Lappe-Siefke et al., 2003); however, unlike our present studies, our earlier assessments lacked quantitative analysis of specific morphological criteria and, thus, may not have detected morphological defects. Also, ultrastructural imaging of the processes and of the MTs within them are warranted. For example, ablation of MAP2, which is essential for dendrite elongation, results in decreased MT density in dendrites (Harada et al., 2002). Finally, it is also conceivable that alternative mechanisms involving other tubulin-interacting/MT assembly proteins may functionally compensate for CNP deficiency during development, as was shown for τ (Takei et al., 2000). One possible candidate that might offset CNP loss is CRMP2, which, interestingly, is expressed in OLs in developing and adult brains (Ricard et al., 2000; Taylor et al., 2004). If such compensatory mechanisms exist during development, these might be absent in adult OLs, thereby leading to abnormal MT organization and to the development of paranodal defects.

Materials and methods

Antibodies

The following mAbs and pAbs were used in this study: CNP mAb (Sternberger); CNP pAb (R422; affinity purified); G-actin, α-tubulin, and β-tubulin mAbs (ICN Biomedicals); His and GST tag mAbs (GE Healthcare); tubulin pAb (Santa Cruz Biotechnology, Inc.); control IgG, acetylated tubulin, and tyrosinated tubulin mAbs (Sigma-Aldrich); τ T49 mAb (gift of V. Lee, University of Pennsylvania School of Medicine, Philadelphia, PA); myelin basic protein pAb (gift of D. Colman, Montreal Neurological Institute, Montreal, Quebec); and rhodamine-labeled phalloidin, goat anti–mouse AlexaFluor594, and goat anti–rabbit AlexaFluor488 (Molecular Probes).

Plasmid constructs

RcRSV-CNP was described previously (De Angelis and Braun, 1994). For high expression, RcCMV was initially constructed from RcRSV vector (Invitrogen) by replacing the entire RSV promoter with the CMV promoter that was obtained from pEGFP-C1 plasmid (CLONTECH Laboratories, Inc.). CNP1, C397S, and CNPΔ13 cDNAs were then subcloned into RcCMV vector. For GFP transfection, pEGFP-N1 (CLONTECH Laboratories, Inc.) was used. The cDNAs encoding rat CNP1 full length (residues 1–400), CNP NH_2-terminal region (residues 1–158), and CNP-CF (residues 150–400) were PCR amplified and subcloned into pGEX-3X (GE Healthcare) and pET15b (Novagen). The cDNAs encoding COOH-terminal deleted CNP mutants (Δ7, Δ13, Δ20, and Δ22) were PCR amplified and subcloned into pET15b. CNP mutants (K379A, G380A, KG-AA, and ΔKG) were constructed using the QuikChange Site-Directed Mutagenesis Kit (Stratagene), after which mutant CNP cDNAs were subcloned into RcCMV-CNP1 for transfection studies.

Cell culture

OLN-93 was a gift from Z.-C. Xiao (Singapore General Hospital, Singapore). All cells were cultured in DME supplemented with 10% FCS, 2 mM L-glutamine, and 100 U/ml penicillin/streptomycin. For transient transfections, cells were plated on coverslips, and dishes were coated with matrigel (1:40 dilution; CLONTECH Laboratories, Inc.) and were transfected using FuGENE 6 (Roche). Cells were transfected for 24–36 h before analysis.

Primary OL cultures

Primary cultures of neonatal rat OLs were prepared from 2-d-old brains (cerebral hemispheres) and purified as described previously (Almazan et al., 1993). OL precursors in serum-free defined medium (Gard and Pfeiffer, 1989) were plated on poly-D-lysine/matrigel-coated surfaces. After plating, synchronized OL populations were obtained after growth conditions that were optimized previously (Bansal and Pfeiffer, 1997): 2 d with 10 ng/ml PDGF-AA and basic fibroblast growth factor, an additional 4 d with 10 ng/ml basic fibroblast growth factor, and up to an additional 8 d in serum-free defined medium without any growth factors. These growth phases enriched for early progenitors, late progenitors, and mature OLs, respectively.

Primary cultures of adult mouse OLs were prepared from 3-mo-old wild-type and CNP-null mice according to a Percoll gradient centrifugation and differential adhesion procedure (Oh et al., 1999). Purified OLs were plated on poly-L-ornithine–coated glass coverslips and cultured in MEM supplemented with 5% FCS and 0.1% dextrose. After plating, cells were treated with 50 ng/ml PMA for 48 h to promote process extension. After treatment, cells were incubated in normal medium for 5 d before analysis. Cells were double stained for myelin basic protein (to identify OLs) and CNP.

Immunofluorescence

Cells were fixed with 4% PFA in PBS before permeabilization in 0.1% Triton X-100 and blocking with 3% BSA in PBS. For detergent extraction before fixation, cells were extracted with 37°C prewarmed MT-stabilizing buffer (Hank's balanced salt solution with 100 mM Pipes, pH 6.9, 4% Polyethylene Glyco 8000, 1 mM EGTA, and 1 mM $MgCl_2$) containing 1% Triton X-100 for 2 min (Song et al., 2001a). Cells were incubated with primary and secondary antibodies in blocking buffer, and coverslips were mounted in Immumount (Fisher Scientific). F-actin staining of OLs was performed as described previously (Song et al., 2001a). Cells were analyzed using a confocal system (model LSM510; Carl Zeiss MicroImaging, Inc.) mounted on a microscope (Axiovert 100; Carl Zeiss MicroImaging, Inc.) or by conventional fluorescence microscopy. Cell surface area was measured using Image software (Scion). Branch number and lengths were measured using LSM Image Browser software (Carl Zeiss MicroImaging, Inc.).

Protein purification and CNPase assays

Recombinant His-tagged proteins were expressed in BL21-Gold (Stratagene) and purified using Ni^{2+}–nitrilotriacetic acid–agarose (QIAGEN). GST-tagged proteins were expressed in BL21 and were purified using glutathione–Sepharose beads (GE Healthcare). GST tag was cleaved from

CNP using Factor Xa (Roche). His tag was cleaved from CNP using thrombin (Calbiochem; Kozlov et al., 2003). To quantitate CNP levels, enzymatic assays were performed as described previously (Lee et al., 2001). Tubulin was isolated from bovine brain by three cycles of assembly/disassembly followed by phosphocellulose ion exchange purification and storage at −80°C in PEM buffer (50 mM Pipes, pH 6.8, 1 mM EGTA, and 1 mM $MgCl_2$) containing 0.5 mM GTP (Williams and Lee, 1982). Purified tubulin preparations contained no MAPs. τ in the purified MAP fraction that was obtained from the tubulin purification procedure was used for biochemical studies. Bovine brain tubulin and rhodamine-labeled tubulin was purchased from Cytoskeleton, Inc. Tubulin concentrations are expressed relative to heterodimers.

Immunoprecipitation

To prepare antibody cross-linked beads, mAbs for CNP, tubulin, and control IgG (100 μl ascites) were diluted with PBS to 2–3 mg/ml and were incubated with 200 μl protein G–Sepharose beads (GE Healthcare) for 3 h at 22°C. Beads were washed with 100 mM Na-borate, pH 8.6, and cross-linked with 2 bed vol of 30 mM dimethylpimelimidate in 0.2 M triethylanolamine for 30 min before quenching the reaction by washing beads several times with 0.2 M ethanolamine and further incubation for 1 h. Cross-linked beads were washed with PBS, and nonlinked antibodies were removed by incubation in low pH buffer (50 mM glycine, pH 2.5, and 0.1% NP-40) for 5 min at RT. Beads were washed in PBS and reused several times for immunoprecipitation experiments by regenerating beads with low pH buffer.

For metabolic labeling experiments, mature OLs in 100-mm dishes were starved for 30 min in cysteine/methionine-free medium and labeled with 4 ml of 0.4 mCi [^{35}S]methionine/cysteine for 3 h. Cells were washed and lysed with 500 μl buffer A (50 mM Hepes, pH 7, 0.15 M NaCl, 1% Triton X-100, 1 mM EDTA, 1 mM PMSF, and 10 μg/ml leupeptin, pepstatin A, and aprotinin) for 30 min at 4°C. Lysates were briefly sonicated and centrifuged 30 min at 13,000 *g*. Extracts were precleared with 50 μl of protein G–Sepharose beads for 1 h before binding to 20 μl of cross-linked CNP or control mAb beads overnight. Immunoprecipitates were washed with buffer A containing 500 mM NaCl and eluted with 150 μl low pH buffer for 5 min at RT. Eluates were adjusted to pH 7.0 and were methanol precipitated. Pellets were resuspended in SDS sample buffer, separated on 4–15% sucrose gradient or 7% SDS-PAGE gels, and visualized by autoradiography.

To identify CNP-interacting proteins, fresh adult whole brains from a single rat or three mice were homogenized at 2,000 rpm in a glass/Teflon homogenizer (10 strokes) in 16 ml buffer A without detergent. 1% Triton X-100 was added, and tissues were again similarly homogenized and incubated at 4°C for 30 min. Tissues were briefly sheared using a POLYTRON homogenizer (Brinkmann Instruments) and centrifuged at 48,000 *g* for 20 min. Soluble brain extracts were filtered through a 0.45-μm syringe filter to remove insoluble material and precleared of nonspecific binding proteins by 1 h incubation with protein G–Sepharose beads (100 μl beads/1 ml extract). For immunoprecipitation under denaturing conditions, 1% SDS was added to detergent-soluble extracts and boiled for 5 min before 10-fold dilution with buffer A and preclearing. Precleared extracts were incubated with 100 μl cross-linked CNP, β-tubulin, or control mAb beads for 4 h or overnight binding. Immunoprecipitates were washed with buffer A and eluted with low pH buffer. For β-tubulin immunoprecipitation, brain extracts were reimmunoprecipitated three times and pooled. Methanol-precipitated proteins were resuspended in SDS sample buffer, separated on 4–15% sucrose gradient or 7% SDS-PAGE gels, and visualized by Coomassie or silver staining or analyzed by immunoblotting.

Tubulin/MT-binding assays

Recombinant GST-CNP proteins were incubated with tubulin or preassembled MTs and glutathione–Sepharose beads in binding buffer (20 mM Tris-HCl, pH 7.5, 150 mM NaCl, 0.1% Triton X-100, 1 mM DTT, and 0.5 mg/ml BSA) for 2 h at 4°C. To compare tubulin with MT binding, preassembled MTs contained 10 μM taxol, and binding was performed at 22°C. Beads were washed with binding buffer, and bound proteins were eluted with SDS sample buffer and were analyzed. Preassembled MTs were prepared by incubating 1.4 mg/ml tubulin in assembly buffer (PEM buffer with 1 mM GTP and DTT) at 37°C with 0.3, 3, and 30 μM taxol after each 10-min interval. Samples were airfuge pelleted through an equal volume of 4 M glycerol cushion in assembly buffer for 15 min at 100,000 *g* at 22°C. MT pellet was resuspended in warm 30 μM taxol assembly buffer. After an additional pelleting step, MTs were verified for its enrichment in the pellet. To assess CNP and τ binding to preassembled MTs, proteins were incubated with MTs for 15 min at 37°C. Samples were pelleted through an equal volume of glycerol cushion, and MT pellets were analyzed by immunoblotting. To assess CNP and τ binding to tubulin, tubulin-preloaded beads were initially prepared by immunoprecipitating 9 μM of purified tubulin with tubulin pAb on protein G–Sepharose beads. Washed tubulin beads were mixed with GST-CNP or τ in binding buffer for 1 h at 22°C, washed, and analyzed. Binding constants were calculated using nonlinear regression analysis (SigmaPlot; Systat Software, Inc.).

MT polymerization assays

For light scattering assays, purified tubulin was mixed with recombinant CNP in assembly buffer to a 100-μl final volume in a small chambered quartz cuvette, and OD_{350} absorbances were monitored at 22°C. For MT sedimentation assays, recombinant CNP was incubated with purified tubulin in assembly buffer at 37°C for 1 h. Samples were pelleted through an equal volume of glycerol cushion for 10 min at 100,000 *g* at 22°C. Supernatants and pellets were analyzed by immunoblotting. To visualize assembled MTs, unlabeled tubulin and rhodamine-labeled tubulin were premixed at a 1:1 ratio to a final concentration of 2 mg/ml in assembly buffer and were stored on ice. CNP was added to an equal volume of tubulin and incubated at 37°C for 30 min. Reactions were diluted and gently mixed in an equal volume of PEM buffer containing 4 M glycerol. Aliquots were plated on a glass slide and were viewed immediately by fluorescence microscopy. For later viewing, 1% glutaraldehyde was included in the dilution buffer, and coverslips were edged with Immumount to prevent drying. His tag–cleaved CNP promoted MT assembly in all assays. His tag–cleaved CNP mutants (K379A, G380A, KG-AA, and ΔKG) were assessed for assembly activity by light scattering assays.

GTP hydrolysis assays

Tubulin was preincubated with 50 μM [γ-^{32}P]GTP (~7,000 cpm/pmol) in assembly buffer for 1 h on ice to allow radiolabeled GTP exchange before initiating the reaction by adding His-CNP to a final volume of 50 μl. Reactions were incubated at 37°C for 15-min intervals, and 10-μl aliquots were used for extraction. Radiolabeled inorganic phosphate release was measured by liquid scintillation counting.

Online supplemental material

Online supplemental material describes how F-actin barriers attenuate CNP-induced process extension in HeLa S3 cells. Fig. S1 shows that CNP-assembled MTs exhibit increased GTP hydrolysis activity. Fig. S2 shows that CNP colocalizes with tubulin/MTs in immature OLs. Fig. S3 shows the effect of CNP overexpression in HeLa S3 cells. Fig. S4 shows that CNP overexpression in HeLa S3 cells promotes process formation after cytochalasin treatment. Online supplemental material is available at http://www.jcb.org/cgi/content/full/jcb.200411047/DC1.

We sincerely thank Dr. Peter Brophy for critical review of the manuscript.

This work was supported by a grant from the Canadian Institutes of Health Research (CIHR). John Lee was a recipient of a studentship from the CIHR and the Fonds pour la Formation de Chercheurs et l'Aide à la Recherche. The authors have no commercial affiliations or conflicts of interest.

Submitted: 8 November 2004
Accepted: 1 July 2005

References

Akum, B.F., M. Chen, S.I. Gunderson, G.M. Riefler, M.M. Scerri-Hansen, and B.L. Firestein. 2004. Cypin regulates dendrite patterning in hippocampal neurons by promoting microtubule assembly. *Nat. Neurosci.* 7:145–152.

Almazan, G., D.E. Afar, and J.C. Bell. 1993. Phosphorylation and disruption of intermediate filament proteins in oligodendrocyte precursor cultures treated with calyculin A. *J. Neurosci. Res.* 36:163–172.

Baas, P.W. 2002. Microtubule transport in the axon. *Int. Rev. Cytol.* 212:41–62.

Bansal, R., and S.E. Pfeiffer. 1997. FGF-2 converts mature oligodendrocytes to a novel phenotype. *J. Neurosci. Res.* 50:215–228.

Baorto, D.M., W. Mellado, and M.L. Shelanski. 1992. Astrocyte process growth induction by actin breakdown. *J. Cell Biol.* 117:357–367.

Bifulco, M., C. Laezza, S. Stingo, and J. Wolff. 2002. 2',3'-Cyclic nucleotide 3'-phosphodiesterase: a membrane-bound, microtubule-associated protein and membrane anchor for tubulin. *Proc. Natl. Acad. Sci. USA.* 99:1807–1812.

Braun, P.E., J. Lee, and M. Gravel. 2004. 2',3'-Cyclic nucleotide 3'-phosphodiesterase: structure, biology, and function. *In* Myelin Biology and Disorders. Vol. 1. R.A. Lazzarini, editor. Elsevier Academic Press, San Diego. 499–522.

Caudron, N., I. Arnal, E. Buhler, D. Job, and O. Valiron. 2002. Microtubule nucleation from stable tubulin oligomers. *J. Biol. Chem.* 277:50973–50979.

De Angelis, D.A., and P.E. Braun. 1994. Isoprenylation of brain 2',3′-cyclic nucleotide 3′-phosphodiesterase modulates cell morphology. *J. Neurosci. Res.* 39:386–397.

De Angelis, D.A., and P.E. Braun. 1996. 2',3′-Cyclic nucleotide 3′-phosphodiesterase binds to actin-based cytoskeletal elements in an isoprenylation-independent manner. *J. Neurochem.* 67:943–951.

Dyer, C.A., and J.A. Benjamins. 1989. Organization of oligodendroglial membrane sheets. I: Association of myelin basic protein and 2',3′-cyclic nucleotide 3′-phosphohydrolase with cytoskeleton. *J. Neurosci. Res.* 24:201–211.

Edson, K., B. Weisshaar, and A. Matus. 1993. Actin depolymerisation induces process formation on MAP2-transfected non-neuronal cells. *Development.* 117:689–700.

Fukata, Y., T.J. Itoh, T. Kimura, C. Menager, T. Nishimura, T. Shiromizu, H. Watanabe, N. Inagaki, A. Iwamatsu, H. Hotani, and K. Kaibuchi. 2002. CRMP-2 binds to tubulin heterodimers to promote microtubule assembly. *Nat. Cell Biol.* 4:583–591.

Gard, A.L., and S.E. Pfeiffer. 1989. Oligodendrocyte progenitors isolated directly from developing telencephalon at a specific phenotypic stage: myelinogenic potential in a defined environment. *Development.* 106:119–132.

Gillespie, C.S., R. Wilson, A. Davidson, and P.J. Brophy. 1989. Characterization of a cytoskeletal matrix associated with myelin from rat brain. *Biochem. J.* 260:689–696.

Gravel, M., J. Peterson, V.W. Yong, V. Kottis, B. Trapp, and P.E. Braun. 1996. Overexpression of 2',3′-cyclic nucleotide 3′-phosphodiesterase in transgenic mice alters oligodendrocyte development and produces aberrant myelination. *Mol. Cell. Neurosci.* 7:453–466.

Gustke, N., B. Trinczek, J. Biernat, E.M. Mandelkow, and E. Mandelkow. 1994. Domains of tau protein and interactions with microtubules. *Biochemistry.* 33:9511–9522.

Harada, A., J. Teng, Y. Takei, K. Oguchi, and N. Hirokawa. 2002. MAP2 is required for dendrite elongation, PKA anchoring in dendrites, and proper PKA signal transduction. *J. Cell Biol.* 158:541–549.

Klein, C., E.M. Kramer, A.M. Cardine, B. Schraven, R. Brandt, and J. Trotter. 2002. Process outgrowth of oligodendrocytes is promoted by interaction of fyn kinase with the cytoskeletal protein tau. *J. Neurosci.* 22:698–707.

Kozlov, G., J. Lee, D. Elias, M. Gravel, P. Gutierrez, I. Ekiel, P.E. Braun, and K. Gehring. 2003. Structural evidence that brain cyclic nucleotide phosphodiesterase is a member of the 2H phosphodiesterase superfamily. *J. Biol. Chem.* 278:46021–46028.

Laezza, C., J. Wolff, and M. Bifulco. 1997. Identification of a 48-kDa prenylated protein that associates with microtubules as 2',3′-cyclic nucleotide 3′-phosphodiesterase in FRTL-5 cells. *FEBS Lett.* 413:260–264.

Lafont, F., M. Rouget, A. Rousselet, C. Valenza, and A. Prochiantz. 1993. Specific responses of axons and dendrites to cytoskeleton perturbations: an in vitro study. *J. Cell Sci.* 104:433–443.

Lappe-Siefke, C., S. Goebbels, M. Gravel, E. Nicksch, J. Lee, P.E. Braun, I.R. Griffiths, and K.A. Nave. 2003. Disruption of Cnp1 uncouples oligodendroglial functions in axonal support and myelination. *Nat. Genet.* 33:366–374.

Lee, J., M. Gravel, E. Gao, R.C. O'Neill, and P.E. Braun. 2001. Identification of essential residues in 2',3′-cyclic nucleotide 3′-phosphodiesterase. Chemical modification and site-directed mutagenesis to investigate the role of cysteine and histidine residues in enzymatic activity. *J. Biol. Chem.* 276:14804–14813.

Lunn, K.F., P.W. Baas, and I.D. Duncan. 1997. Microtubule organization and stability in the oligodendrocyte. *J. Neurosci.* 17:4921–4932.

Luo, L. 2002. Actin cytoskeleton regulation in neuronal morphogenesis and structural plasticity. *Annu. Rev. Cell Dev. Biol.* 18:601–635.

Maccioni, R.B., and V. Cambiazo. 1995. Role of microtubule-associated proteins in the control of microtubule assembly. *Physiol. Rev.* 75:835–864.

Oh, L.Y., and V.W. Yong. 1996. Astrocytes promote process outgrowth by adult human oligodendrocytes in vitro through interaction between bFGF and astrocyte extracellular matrix. *Glia.* 17:237–253.

Oh, L.Y., P.H. Larsen, C.A. Krekoski, D.R. Edwards, F. Donovan, Z. Werb, and V.W. Yong. 1999. Matrix metalloproteinase-9/gelatinase B is required for process outgrowth by oligodendrocytes. *J. Neurosci.* 19:8464–8475.

Pereyra, P.M., E. Horvath, and P.E. Braun. 1988. Triton X-100 extractions of central nervous system myelin indicate a possible role for the minor myelin proteins in the stability in lamellae. *Neurochem. Res.* 13:583–595.

Rasband, M.N., J. Tayler, Y. Kaga, Y. Yang, C. Lappe-Siefke, K.A. Nave, and R. Bansal. 2005. CNP is required for maintenance of axon-glia interactions at nodes of Ranvier in the CNS. *Glia.* 50:86–90.

Ricard, D., B. Stankoff, D. Bagnard, M. Aguera, V. Rogemond, J.C. Antoine, N. Spassky, B. Zalc, C. Lubetzki, M.F. Belin, and J. Honnorat. 2000. Differential expression of collapsin response mediator proteins (CRMP/ULIP) in subsets of oligodendrocytes in the postnatal rodent brain. *Mol. Cell. Neurosci.* 16:324–337.

Richter-Landsberg, C. 2001. Organization and functional roles of the cytoskeleton in oligodendrocytes. *Microsc. Res. Tech.* 52:628–636.

Salzer, J.L. 2003. Polarized domains of myelinated axons. *Neuron.* 40:297–318.

Scherer, S.S., P.E. Braun, J. Grinspan, E. Collarini, D.Y. Wang, and J. Kamholz. 1994. Differential regulation of the 2',3′-cyclic nucleotide 3′-phosphodiesterase gene during oligodendrocyte development. *Neuron.* 12:1363–1375.

Shah, J.V., and D.W. Cleveland. 2002. Slow axonal transport: fast motors in the slow lane. *Curr. Opin. Cell Biol.* 14:58–62.

Song, J., B.D. Goetz, P.W. Baas, and I.D. Duncan. 2001a. Cytoskeletal reorganization during the formation of oligodendrocyte processes and branches. *Mol. Cell. Neurosci.* 17:624–636.

Song, J., B.D. Goetz, S.L. Kirvell, A.M. Butt, and I.D. Duncan. 2001b. Selective myelin defects in the anterior medullary velum of the taiep mutant rat. *Glia.* 33:1–11.

Takei, Y., J. Teng, A. Harada, and N. Hirokawa. 2000. Defects in axonal elongation and neuronal migration in mice with disrupted τ and map1b genes. *J. Cell Biol.* 150:989–1000.

Taylor, C.M., C.B. Marta, R.J. Claycomb, D.K. Han, M.N. Rasband, T. Coetzee, and S.E. Pfeiffer. 2004. Proteomic mapping provides powerful insights into functional myelin biology. *Proc. Natl. Acad. Sci. USA.* 101:4643–4648.

Teng, J., Y. Takei, A. Harada, T. Nakata, J. Chen, and N. Hirokawa. 2001. Synergistic effects of MAP2 and MAP1B knockout in neuronal migration, dendritic outgrowth, and microtubule organization. *J. Cell Biol.* 155:65–76.

Terada, S. 2003. Where does slow axonal transport go? *Neurosci. Res.* 47:367–372.

Terada, S., M. Kinjo, and N. Hirokawa. 2000. Oligomeric tubulin in large transporting complex is transported via kinesin in squid giant axons. *Cell.* 103:141–155.

Williams, R.C., Jr., and J.C. Lee. 1982. Preparation of tubulin from brain. *Methods Enzymol.* 85:376-85.

Wilson, R., and P.J. Brophy. 1989. Role for the oligodendrocyte cytoskeleton in myelination. *J. Neurosci. Res.* 22:439–448.

Yin, X., J. Peterson, M. Gravel, P.E. Braun, and B.D. Trapp. 1997. CNP overexpression induces aberrant oligodendrocyte membranes and inhibits MBP accumulation and myelin compaction. *J. Neurosci. Res.* 50:238–247.

Yong, V.W., J.C. Cheung, J.H. Uhm, and S.U. Kim. 1991. Age-dependent decrease of process formation by cultured oligodendrocytes is augmented by protein kinase C stimulation. *J. Neurosci. Res.* 29:87–99.

Yu, W., V.E. Centonze, F.J. Ahmad, and P.W. Baas. 1993. Microtubule nucleation and release from the neuronal centrosome. *J. Cell Biol.* 122:349–359.